

# Differential effects of TRPM4 channel inhibitors on Guinea pig urinary bladder smooth muscle excitability and contractility: Novel 4-chloro-2-[2-(2-chloro-phenoxy)-acetylamino]-benzoic acid (CBA) versus classical 9-phenanthrol

John Malysz  | Sarah E. Maxwell  | Georgi V. Petkov 

Department of Pharmaceutical Sciences,  
College of Pharmacy, University of  
Tennessee Health Science Center,  
Memphis, Tennessee, USA

## Correspondence

John Malysz and Georgi V. Petkov,  
Department of Pharmaceutical Sciences,  
College of Pharmacy, University of  
Tennessee Health Science Center,  
Pharmacy Bldg., Room 551, 881 Madison  
Avenue, Memphis, TN 38163, USA.  
Email: jmalysz@unr.edu; jmalysz@uthsc.edu  
and gpetkov@uthsc.edu

## Present address

John Malysz, Department of Physiology  
and Cell Biology, University of Nevada,  
Reno, Nevada, USA

## Funding information

National Institute of Diabetes and  
Digestive and Kidney Diseases, Grant/  
Award Number: P20 DK-123971 and  
R01 DK-106964

## Abstract

Non-selective cation channels in urinary bladder smooth muscle (UBSM) are thought to mediate increases in cellular excitability and contractility. For transient receptor potential melastatin type-4 (TRPM4) channels, the evidence primarily relies on the inhibitor 9-phenanthrol, which exhibits pharmacological limitations. Recently, 4-chloro-2-[2-(2-chloro-phenoxy)-acetylamino]-benzoic acid (CBA) has been discovered as a novel TRPM4 channel blocker. We examined how, in comparison to 9-phenanthrol, CBA affects the excitability of freshly isolated guinea pig UBSM cells and the contractility of UBSM strips. Additionally, non-selective TRPM4 channel inhibitor flufenamic acid (FFA) and potentiator BTP2 (also known as YM-58483) were studied in UBSM cells. Unlike robust inhibition for 9-phenanthrol already known, CBA (up to 100  $\mu$ M) displayed either no or a very weak reduction (<20%) in spontaneous phasic, 20 mM KCl-induced, and electrical field stimulated contractions. For 300  $\mu$ M CBA, reductions were higher except for an increase in the frequency of KCl-induced contractions. In UBSM cells, examined under amphotericin B-perforated patch-clamp, CBA (30  $\mu$ M) did not affect the membrane potential ( $I = 0$ ) or voltage step-induced whole-cell cation currents, sensitive to 9-phenanthrol. The currents were not inhibited by FFA (100  $\mu$ M), increased by BTP2 (10  $\mu$ M), nor enhanced under a strongly depolarizing holding voltage of  $-16$  or  $+6$  mV (vs.  $-74$  mV). None of the three compounds affected the cell capacitance, unlike 9-phenanthrol. In summary, the novel inhibitor CBA and nonselective FFA did not mimic the inhibitory properties of 9-phenanthrol on UBSM function. These results suggest that TRPM4 channels, although expressed in UBSM, play a distinct role rather than direct regulation of excitability and contractility.

**Abbreviations:** BTP2, N-[4-[3,5-Bis(trifluoromethyl)pyrazol-1-yl]phenyl]-4-methylthiadiazole-5-carboxamide, alias YM-58483;  $Ca_v$ , voltage-gated  $Ca^{2+}$  (channel); CBA, 4-chloro-2-[2-(2-chloro-phenoxy)-acetylamino]-benzoic acid; ddH<sub>2</sub>O, double distilled H<sub>2</sub>O; EFS, electrical field stimulation; FFA, flufenamic acid; IK, intermediate conductance calcium activated K<sup>+</sup> (channel);  $K_{Ca}$ 1.1, voltage and calcium activated large conductance K<sup>+</sup> (channel), alias BK or MaxiK<sup>+</sup>;  $K_v$ , voltage-gated K<sup>+</sup> (channel);  $Na_v$ , voltage-gated Na<sup>+</sup> (channel); UBSM, urinary bladder smooth muscle; TRPM4, transient receptor potential melastatin type-4.

This is an open access article under the terms of the [Creative Commons Attribution](https://creativecommons.org/licenses/by/4.0/) License, which permits use, distribution and reproduction in any medium, provided the original work is properly cited.

© 2022 The Authors. *Pharmacology Research & Perspectives* published by British Pharmacological Society and American Society for Pharmacology and Experimental Therapeutics and John Wiley & Sons Ltd.

## KEYWORDS

bladder, contraction coupling, patch clamp, smooth muscle, transient receptor potential channels

## 1 | INTRODUCTION

Urinary bladder smooth muscle (UBSM) relaxation and contraction determine urine storage or voiding, respectively.<sup>1</sup> UBSM cells express various types of ion channels that either inhibit (e.g., voltage-dependent K<sup>+</sup> channel type 2 or *K<sub>v</sub>2*, *K<sub>v</sub>7*, and *K<sub>Ca</sub>1.1*) or promote (e.g., voltage-gated Ca<sup>2+</sup> channel type 1.2 or *Ca<sub>v</sub>1.2* and *Ca<sub>v</sub>3*) cell excitability.<sup>2</sup> Seminal studies on guinea pigs<sup>3</sup> and rats<sup>4</sup> and later on humans<sup>5</sup> and mice<sup>6,7</sup> identified the transient receptor potential melastatin type-4 (*TRPM4*) channel as a likely regulator of UBSM excitation-contraction coupling.

Unlike most TRP channels, TRPM4 channels exhibit high selective permeability to only monovalent cations (Na<sup>+</sup> and K<sup>+</sup>) but not to divalent cations like Ca<sup>2+</sup> and Mg<sup>2+</sup>, or anions.<sup>8-10</sup> Intracellular Ca<sup>2+</sup> activates TRPM4 channels, whereas ATP inhibits them, thus linking intracellular signaling and metabolism to channel regulation.<sup>8-10</sup> In the case of smooth muscle cells including UBSM cells, the opening of cell membrane TRPM4 channels is thought to induce depolarization, causing subsequent opening of Ca<sub>v</sub> channels, net Ca<sup>2+</sup> influx, increase in intracellular Ca<sup>2+</sup>, and activation of contractile machinery.<sup>3-5,11,12</sup>

Two major lines of evidence have been provided for the role of TRPM4 channels in UBSM function. First, UBSM tissues and cells showed robust expression of TRPM4 mRNA and protein.<sup>3-5,7,12,13</sup> Second, 9-phenanthrol, a widely used TRPM4 channel inhibitor,<sup>14</sup> caused attenuation of UBSM cell excitability and inhibition of contractility in UBSM strips.<sup>3-7,12,13,15</sup> The presence of TRPM4 channels and pharmacological studies using TRPM4 channel modulators, especially 9-phenanthrol, have also revealed a role of TRPM4 channels in insulin secretion (pancreatic β-cells), cardiac excitability (ventricular cells), immune response (lymphocytes and monocytes), and vascular smooth muscle excitability and contractility.<sup>10,11,16-18</sup> 9-Phenanthrol, hence, has been a key compound in investigating TRPM4 channels in various cell types.<sup>14</sup>

Pharmacologically, 9-phenanthrol shows modest potency (IC<sub>50</sub>) of ~15–30 μM for TRPM4 channels expressed in human embryonic kidney (HEK)-293 cells determined electrophysiologically or with an imaging assay utilizing a Na<sup>+</sup>-sensitive dye.<sup>19,20</sup> In experiments on native cells, the tested concentration is typically in the range of 10–100 μM. In UBSM cells, the most effective concentration is 100 μM with some non-specific effects most likely occurring due to loss of cell viability at higher concentrations.<sup>15</sup> Selectivity of 9-phenanthrol for TRPM4 channels is not optimum. When tested at 10–100 μM, 9-phenanthrol has been reported to also block *TMEM16A*/Ano1 Cl<sup>-</sup>, Ca<sub>v</sub>, Na<sub>v</sub>, K<sub>v</sub>, and IK currents and to induce cytotoxicity.<sup>21-25</sup> The limitations of 9-phenanthrol including its poor aqueous solubility have led to the need of discovering more selective TRPM4 channel inhibitors. One such compound recently identified is *CBA*.

*CBA* inhibits TRPM4 channels with a 20-fold greater potency than 9-phenanthrol.<sup>20</sup> Other modulators, albeit non-selective, used to study TRPM4 channels are flufenamic acid (FFA) and *BTP2* (also known as YM-58483), which, respectively, block and potentiate them.<sup>20,26,27</sup>

In this study, we aimed to further corroborate the role of TRPM4 channels in UBSM excitability and contractility using the novel TRPM4 channel inhibitor, *CBA*, and two other known modulators, the activator *BTP2* and inhibitor FFA, in guinea pig UBSM. We found unexpectedly that *CBA* and FFA did not mimic the inhibitory effect of 9-phenanthrol nor did we observe any change for *BTP2* on UBSM excitability. We elaborate on the implications of these novel findings regarding TRPM4 channel function in UBSM.

## 2 | MATERIALS AND METHODS

### 2.1 | UBSM tissue harvesting

Experiments were conducted in accordance with the Animal Use Protocols No. 17-075 and 20-019 reviewed and approved by the University of Tennessee Health Science Center (Memphis, TN). For this study, 31 adult male Hartley-Albino guinea pigs (median weight: 662g, 25th percentile: 538g; 75th percentile: 931g) were euthanized either with CO<sub>2</sub> or isoflurane (Forane<sup>®</sup>, Baxter, Deerfield, IL) followed by thoracotomy. Then, the whole bladder was cut above the bladder neck and transferred to a Petri dish containing dissection/digestion solution (see *Solutions and compounds* section for composition). The whole bladder was excised, and the mucosa including urothelium removed. UBSM strips (5–10mm long and 2–4mm wide) were prepared for isometric tension recordings and for UBSM single-cell isolation.

### 2.2 | Fresh enzymatic single UBSM cell isolation

Guinea pig UBSM cells were isolated as previously described.<sup>3,15</sup> Briefly, small UBSM strips were cut from the mucosa-free UBSM specimens and placed in dissection/digestion solution (1–2 ml) supplemented with 1 mg/ml bovine serum albumin (BSA), 1–1.5 mg/mL papain, and 1 mg/mL dithiothreitol and incubated for 15–35 min at ~37°C. Next, UBSM strips were transferred to dissection solution (1–2 ml) containing 1 mg/mL BSA, 1–2 mg/mL type II collagenase, and 100–200 μM CaCl<sub>2</sub> for 15–35 min at ~37°C. After the incubation, UBSM strips were washed with fresh dissection/digestion solution containing BSA. Individual UBSM cells were released from the tissue by passing through a Pasteur pipette. UBSM cells were immediately used in electrophysiological patch-clamp recordings or stored at –4°C for further use within 6 h.

## 2.3 | Electrophysiological experiments

Amphotericin B-perforated whole-cell patch-clamp recordings were performed based on methods and procedures previously described.<sup>3,15,28</sup> Briefly, several drops of the dissection/digestion solution containing freshly isolated UBSM cells were placed into a recording chamber. After at least 45 min, the cells were washed several times with the extracellular (bath) solution (see *Solutions and compounds*). Voltage step-induced currents or membrane potentials (current clamp,  $I = 0$ ) were recorded using an Axopatch 200B amplifier, Digidata 1440A, and pCLAMP version 10 software (Molecular Devices, Union City, CA) and solutions optimized for the recording of cation currents ( $K^+$  currents minimized, see *Solutions and compounds*). The patch-clamp pipettes were prepared from borosilicate glass (Sutter Instruments, Novato, CA) and pulled using a Sutter P-97 horizontal puller (Sutter Instrument Co., Novato, CA). Pipettes were fire-polished with a Microforge MF-830 (Narishige Group, Tokyo, Japan) to give a final tip resistance of approximately 3–6 M $\Omega$ . In perforated voltage-clamp patch-clamp experiments, UBSM cells were held at  $-74$  mV (corrected for the junction potential), voltage-stepped from  $-94$  to  $106$  mV (also corrected for the junction potential) in  $10$  mV increments for  $400$  or  $500$  ms, and returned to  $-74$  mV. Membrane potential recordings were obtained using the current-clamp ( $I = 0$ ) mode and physiological (high  $Na^+$  and  $Cl^-$  in bath and lowered intracellular/pipette  $Cl^-$ ) solutions (see *Solutions and compounds* section); the membrane potential values were corrected for the junction potential. All experiments were carried out at room temperature ( $21$ – $23^\circ C$ ) within the same day of UBSM cell isolation. The maximum concentration of DMSO vehicle to dissolve CBA and 9-phenanthrol did not exceed  $0.2\%$ . At this concentration, DMSO does not affect UBSM function.<sup>29,30</sup>

## 2.4 | Isometric UBSM tension recordings

The isometric UBSM tension recording experiments were conducted as previously described.<sup>3,13,15</sup> Briefly, UBSM strips were clipped between a stationary mount and a force-displacement transducer and then placed in tissue baths filled with  $Ca^{2+}$ -containing physiological salt solution (PSS) thermostatically controlled at  $37^\circ C$ . UBSM strips were stretched to an initial level of  $\sim 10$  mN ( $1$  g) and washed with fresh PSS every  $15$  min for  $45$ – $60$  min equilibration period. For spontaneous and  $20$  mM KCl-induced phasic contractions (obtained by supplying an additional  $15.3$  mM KCl to bath), the neuronal  $Na^+$  channel blocker tetrodotoxin ( $1$   $\mu M$ ) was then added to the baths to attenuate neuronal activity. Once stable contractions developed (following at least  $1$  h equilibration period in the presence of tetrodotoxin) increasing concentrations of CBA were applied cumulatively at  $10$  to  $12$  min intervals on spontaneous or  $20$  mM KCl-induced phasic contractions. In separate experiments, nerve-evoked UBSM contractions

were induced by electrical field stimulation (EFS) using a pair of platinum electrodes mounted in the tissue bath parallel to the UBSM strip. The EFS pulses were generated using a PHM-1521 stimulator (Med Associates, Georgia, VT). The EFS pulse parameters were as follows:  $0.75$ -ms width,  $20$ -V amplitude, and  $3$ -s stimulus duration, with polarity reversed for alternating pulses. For EFS studies, after the equilibration period, UBSM strips were subjected to continuous stimulation with a  $10$  Hz stimulation frequency at  $1$  min intervals and increasing concentrations of CBA were applied cumulatively at  $10$  to  $12$  min intervals. Unlike spontaneous and  $20$  mM KCl-induced phasic contractions, all EFS responses were recorded in the absence of tetrodotoxin ( $1$   $\mu M$ ).

## 2.5 | Solutions and compounds

The dissection/digestion solution with or without supplemented  $Ca^{2+}$  ( $100$ – $200$   $\mu M$ ) had the following composition (in mM):  $80$  monosodium glutamate,  $55$  NaCl,  $6$  KCl,  $10$  glucose,  $10$  HEPES, and  $2$   $MgCl_2$ , pH  $7.3$ , adjusted with NaOH. The  $Ca^{2+}$ -containing PSS for UBSM contractility studies was freshly prepared daily and contained the following (in mM):  $119$  NaCl,  $4.7$  KCl,  $24$   $NaHCO_3$ ,  $1.2$   $KH_2PO_4$ ,  $2.5$   $CaCl_2$ ,  $1.2$   $MgCl_2$ ,  $11$  glucose, and aerated with  $95\%$   $O_2$ – $5\%$   $CO_2$  to obtain pH  $7.4$ . In perforated voltage-clamp experiments to measure the voltage step-induced cation currents, the extracellular (bath) solution contained the following (in mM):  $10$  tetraethylammonium-chloride (TEA-Cl),  $6$  CsCl,  $124$  NaCl,  $1$   $MgCl_2$ ,  $2$   $CaCl_2$ ,  $10$  4-(2-hydroxyethyl)-1-piperazineethanesulfonic acid (HEPES),  $10$  glucose, and  $0.002$ – $0.003$  nifedipine (pH  $7.4$  adjusted with CsOH), and pipette solution supplemented with freshly dissolved  $300$ – $450$   $\mu g/ml$  amphotericin B (in mM):  $110$  CsOH,  $110$  aspartic acid,  $10$  NaCl,  $1$   $MgCl_2$ ,  $10$  HEPES,  $0.05$  ethylene glycol-bis( $\beta$ -aminoethyl ether)- $N,N,N',N'$ -tetraacetic acid (EGTA), and  $30$  CsCl (pH  $7.2$  adjusted with CsOH). Membrane potential recordings were made using the amphotericin B-perforated current-clamp ( $I = 0$ ) in the presence of the following extracellular solution (in mM):  $134$  NaCl,  $6$  KCl,  $1$   $MgCl_2$ ,  $2$   $CaCl_2$ ,  $10$  glucose, and  $10$  HEPES, pH adjusted to  $7.4$  with NaOH; and intracellular pipette solution containing freshly dissolved  $300$ – $450$   $\mu g/mL$  amphotericin B (in mM):  $110$  potassium aspartate,  $30$  KCl,  $10$  NaCl,  $1$   $MgCl_2$ ,  $10$  HEPES, and  $0.05$  EGTA, pH adjusted to  $7.2$  with NaOH. Papain and collagenase type II were bought from Worthington (Lakewood, NJ) or Sigma-Aldrich/Millipore (St. Louis, MO). CBA (cat no: OSSK\_529112) was purchased from Princeton BioMolecular Research, flufenamic acid from Fluka Analytical (Honeywell Fluka™, Charlotte, NC), and BTP2 from Cayman Chemical (Ann Arbor, MI). All other chemicals were obtained from Sigma-Aldrich/Millipore or Fisher Scientific (Pittsburgh, PA). Stock solutions of CBA ( $30$  or  $100$  mM) and nifedipine ( $10$  mM) were prepared in DMSO. Tetrodotoxin (citrate) was dissolved in  $ddH_2O$  at  $1$  mM stock. Compounds were diluted in extracellular solutions and tested at concentrations as specified.

Contraction parameter	CBA	9-Phenanthrol <sup>a</sup>
	IC <sub>50</sub> , Mean (95% CI) Max inhibition, Mean ± SEM (n = 4–9, N = 4–8)	IC <sub>50</sub> , Mean (95% CI) Max inhibition, Mean ± SEM (n = 12, N = 10)
Amplitude	163.8 (95.2–281.7) μM 69.3 ± 15.3%	1.5 (0.4–6.3) μM 73.3 ± 11.5%
Force	130.9 (69.7–245.7) μM 75.6 ± 13.2%	1.1 (0.4–3.2) μM 78.3 ± 9.4%
Duration (Half-Width)	230.2 (161.1–328.9) μM 64.2 ± 17.4%	6.7 (1.4–15.3) μM 70.7 ± 12.7%
Frequency	> 300 μM 33.8 ± 32.9%	10.0 (2.6–49.7) μM 76.4 ± 10.2%
Muscle Tone	339.1 (62.7–1833) μM 58.3 ± 15.2%	1.3 (0.4–4.7) μM 35.1 ± 6.9%

<sup>a</sup>Data for 9-phenanthrol are from Malysz et al.<sup>15</sup>

## 2.6 | Data analyses and statistics

Clampfit software version 10, GraphPad Prism version 8.0 (La Jolla, CA), and Microsoft Excel were used for the analysis of patch-clamp data. Steady-state cation currents for the pre-application controls, in the presence of a test condition either ion substitution or compound addition, and wash-out (if applicable) were analyzed as averages over the last 200ms of each voltage step. The average current values were then divided by the cell capacitance (constantly monitored) to calculate the current densities at each voltage. The responses for all voltages were then normalized to the current density measured at +106 mV for the pre-application control of each cell unless stated otherwise. Analyses determining the effects of compounds on currents were carried out by subtracting the responses (current density values) obtained for a given compound at a voltage step from that of the pre-addition and normalized to the pre-addition control of +106 mV for each cell. Cell capacitance was constantly monitored during the course of the recording. In the case of membrane potential recordings, 3 min intervals prior to and after the addition of CBA for at least 5 min were analyzed as averaged values. Isometric UBSM tension recordings were obtained live with MyoMed software (Med Associates, St. Albans, VT). MiniAnalysis software (Synptosoft, Decatur, GA) was used for data analysis of UBSM phasic contraction amplitude, muscle force integral (determined by integrating the area under the curve of the phasic contractions), frequency, duration (determined at half-width level), and muscle tone over the last 5 min interval before the addition of a higher concentration of CBA. GraphPad Prism 8.0 software (GraphPad Software, La Jolla, CA) or Excel (Microsoft) were used for statistical analyses (including the testing for normal data distribution, ANOVA with a mixed model if applicable, and Student's *t*-tests), and CorelDraw Graphic Suite software (Corel, Ottawa, ON, Canada) or Microsoft PowerPoint (Seattle, WA) for data illustration. The data are summarized as means ± SEM for normally distributed data or median (25th–75th percentiles) for non-normal datasets, *n* = number of UBSM cells or tissue strips;

**TABLE 1** Summary of potency and maximum efficacy values for CBA and 9-phenanthrol on UBSM spontaneous phasic contraction parameters and muscle tone

**TABLE 2** Summary of potency and maximum efficacy values for CBA and 9-phenanthrol on 20mM KCl-induced UBSM phasic contraction parameters and muscle tone

Contraction parameter	CBA	9-Phenanthrol <sup>a</sup>
	IC <sub>50</sub> , Mean (95% CI) Max inhibition, Mean ± SEM (n = 10–17, N = 6–11)	IC <sub>50</sub> , Mean (95% CI) Max inhibition, Mean ± SEM (n = 12, N = 10)
Amplitude	302 (138.7–657.9) μM 58.9 ± 6.4%	8.7 (3.7–20.0) μM 75.7 ± 6.8%
Force	191.9 (97.6–377.4) μM 70.9 ± 5.6%	5.8 (2.7–7.9) μM 81.5 ± 5.0%
Duration (Half-Width)	> 300 μM 42.4 ± 10.4%	21.9 (6.3–75.9) μM 62.0 ± 8.6%
Frequency	> 300 μM –85.1 ± 33.4% <sup>b</sup>	13.3 (4.0–44.4) μM 64.0 ± 10.4%
Muscle tone	> 300 μM 9.3 ± 6.5%	3.4 (0.8–13.9) μM 38.7 ± 6.4%

<sup>a</sup>Data for 9-phenanthrol are from Malysz et al.<sup>15</sup>

<sup>b</sup>Negative response indicates an increase in contractility.

*N* = number of guinea pigs used. Data (*n* values) were compared using two-way ANOVA and paired or unpaired Student's *t*-test as appropriate. A *p* value <.05 (two-tailed for all) was considered statistically significant.

## 2.7 | Nomenclature of targets and ligands

Key protein targets and ligands in this article are hyperlinked to corresponding entries in <http://www.guidetopharmacology.org>, the common portal for data from the IUPHAR/BPS Guide to PHARMACOLOGY,<sup>31</sup> and are permanently archived in the Concise Guide to PHARMACOLOGY 2019/20.<sup>32</sup>

### 3 | RESULTS

#### 3.1 | Differential effects of CBA and 9-phenanthrol on UBSM spontaneous phasic, 20 mM KCl-induced phasic, and EFS-evoked contractions

We have previously shown that 9-phenanthrol, a classical TRPM4 channel blocker, effectively inhibited guinea pig UBSM contractility<sup>3,15</sup>; see also Tables 1–3. Here, we further examined how the novel TRPM4 channel inhibitor CBA affects UBSM contractility in the same animal species. The effects of CBA were examined on spontaneous phasic (Figure 1 and Table 1), 20 mM KCl-induced (Figure 2 and Table 2), and EFS-evoked contractions (Figure 3 and Table 3) over a range of increasing concentrations from 300 nM up to 300  $\mu$ M. For all phasic contraction parameters (amplitude, force, duration, and/or frequency) CBA did not attenuate contractility at concentrations up to and including 30  $\mu$ M. At the highest tested concentrations of CBA, inhibitory effects were observed. For spontaneous phasic contractions, the contraction amplitude and muscle force were maximally decreased by 70%–75% with  $IC_{50}$  values in the range of 130–160  $\mu$ M (Figure 1 and Table 1). Comparable maximum inhibitions were observed for 20 mM KCl-induced contractions with 60%–70% inhibition of both contraction amplitude and muscle force with  $IC_{50}$  values ranging from 200 to 300  $\mu$ M (Table 2). The amplitude and muscle force of EFS-evoked contractions exhibited maximum inhibitions of 40%–50% with  $IC_{50}$  values >300  $\mu$ M (Figure 3 and Table 3). Of note, the frequency for 20 mM KCl-induced phasic contractions, unlike spontaneous phasic and EFS-evoked contractions, increased at the highest concentrations tested (Figure 2A,B and Table 2). The comparison of responses to CBA and 9-phenanthrol on the three types of contractions revealed that the effects of the former compound were substantially weaker (Tables 1–3). The absence of a robust inhibitory effect of CBA on UBSM contractility was surprising given the compound was reported to have ~20-fold higher potency

**TABLE 3** Summary of potency and maximum efficacy values for CBA and 9-phenanthrol on nerve-evoked UBSM contraction parameters

Contraction parameters	CBA	9-Phenanthrol <sup>a</sup>
	$IC_{50}$ , Mean (95% CI) Max inhibition, Mean $\pm$ SEM ( $n = 10$ , $N = 4$ )	$IC_{50}$ , Mean (95% CI) Max inhibition, Mean $\pm$ SEM ( $n = 12$ , $N = 8$ )
Amplitude	393.8 (238.4–735.0) $\mu$ M 50.9 $\pm$ 12.1%	1.8 (1.2–2.6) $\mu$ M 84.7 $\pm$ 3.1%
Force	> 300 $\mu$ M 39.4 $\pm$ 14.9%	1.8 (1.3–2.6) $\mu$ M 84.4 $\pm$ 3.1%
Duration (Half-Width)	> 300 $\mu$ M –5.9 $\pm$ 6.2% <sup>b</sup>	No significant effect
Muscle tone	> 300 $\mu$ M –13.6 $\pm$ 9.0% <sup>b</sup>	No significant effect

<sup>a</sup>Data are from Smith et al.<sup>3</sup>

<sup>b</sup>Negative response indicates an increase in contractility.

and comparable maximum efficacy to 9-phenanthrol for TRPM4 channels.<sup>20</sup>

#### 3.2 | Differential effects of CBA and 9-phenanthrol on the excitability of isolated UBSM cells: Lack of effects of CBA on membrane potential and voltage-step-induced cation currents

9-Phenanthrol effectively hyperpolarizes UBSM cells when measured using the amphotericin B perforated patch-clamp technique.<sup>3</sup> Using the same experimental approach, we performed comparative experiments with CBA. As shown in Figure 4, CBA did not change the membrane potential of UBSM cells. The control membrane potential was  $-25.0 \pm 6.6$  mV ( $n = 7$ ,  $N = 7$ ), which remained comparable in the presence of 30  $\mu$ M CBA,  $\Delta -0.9 \pm 0.5$  mV ( $n = 7$ ,  $N = 7$ ,  $p > .05$ , paired *t*-test). Next, the effect of CBA was examined on voltage-step-induced cation currents. Similar to the observation of the membrane potential, CBA did not cause any change in the voltage-step-induced currents (Figure 5A,B). Of note, the subsequent application of 9-phenanthrol (100  $\mu$ M) in the presence of CBA caused significant inhibition of ~50%–60% at voltages of +56 mV and above up to +106 mV (Figure 5A,B). For example, the normalized responses at +106 mV, were 1 for control,  $0.95 \pm 0.08$  for CBA ( $n = 9$ ,  $N = 7$ ), and  $0.41 \pm 0.06$  for CBA + 9-phenanthrol ( $n = 7$ ,  $N = 6$ ,  $p < .01$  paired *t*-test vs same cells in CBA,  $0.94 \pm 0.10$ ). Upon washout of CBA + 9-phenanthrol, when experimentally possible to maintain UBSM cell recordings, the responses recovered near their control values,  $1.1 \pm 0.1$  ( $n = 6$ ,  $N = 6$ ). During the course of the experiments, the cell capacitance was constantly monitored, and it did not change following the application of CBA (30  $\mu$ M). The cell capacitance values were  $47.5 \pm 7.3$  pF and  $47.5 \pm 7.4$  pF ( $n = 9$ ,  $N = 7$ ) in the absence and presence of CBA, respectively. The addition of 9-phenanthrol (100  $\mu$ M) in the presence of CBA increased the cell capacitance to  $53.2 \pm 9.2$  pF ( $n = 7$ ,  $N = 6$ ;  $p < .05$  vs CBA-only:  $51.1 \pm 10.9$  pF). These experiments illustrate that the two UBSM cell excitability parameters, membrane potential, and voltage-step-induced currents, were unaffected by CBA.

#### 3.3 | Flufenamic acid (FFA), a nonselective TRPM4 channel blocker, does not reduce 9-phenanthrol-sensitive voltage-step-induced cation currents in freshly isolated UBSM cells

FFA, albeit non-selective, has been shown to effectively inhibit TRPM4 channels.<sup>20,26,33</sup> Here, the effect of FFA was evaluated on voltage-step-induced cation currents in UBSM cells. FFA, tested at 100  $\mu$ M, did not inhibit the currents. Instead, an enhancement was noted especially for voltages of +86 mV and higher. For example, at +106 mV the normalized voltage-step-induced current increased from 1 to  $1.41 \pm 0.15$  ( $n = 7$ ,  $N = 7$ ,  $p < .05$ , Sidak multiple comparison post hoc test, Figure 6). The stimulatory effect of FFA

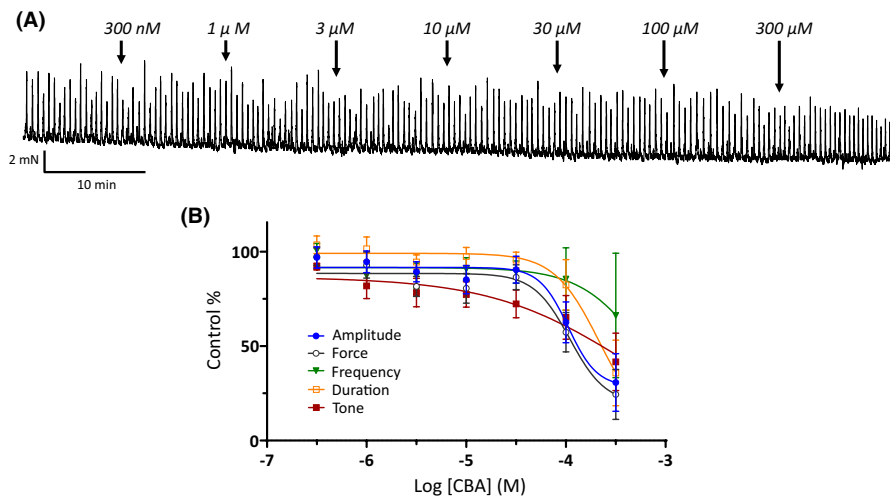


**FIGURE 1** Modest efficacy of the novel TRPM4 channel inhibitor CBA on spontaneous phasic UBSM contractions. (A) Shown is a representative isometric UBSM tension recording demonstrating the effect of cumulative additions of CBA (300 nM to 300 μM) on spontaneous phasic UBSM contractions. (B) Presented are summary concentration-response graphs for CBA on UBSM phasic contraction amplitude, muscle force, duration (half-width), frequency of spontaneous phasic contractions, and muscle tone ( $n = 9$ ,  $N = 8$ ).

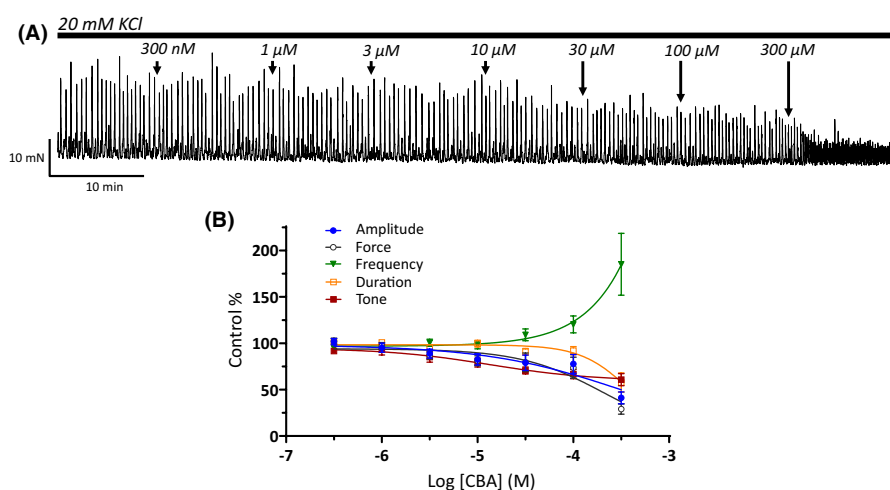


**FIGURE 2** Weak inhibitory effects of CBA on 20 mM KCl-induced phasic UBSM contractions. (A) Shown is a representative isometric UBSM tension recording demonstrating the effect of cumulative additions of CBA (300 nM–300 μM) on 20 mM KCl-induced phasic UBSM contractions. (B) Presented are summary concentration-response graphs for CBA on UBSM phasic contraction amplitude, muscle force, duration (half-width), frequency of 20 mM KCl-induced phasic contractions, and muscle tone ( $n = 17$ ,  $N = 11$ ).

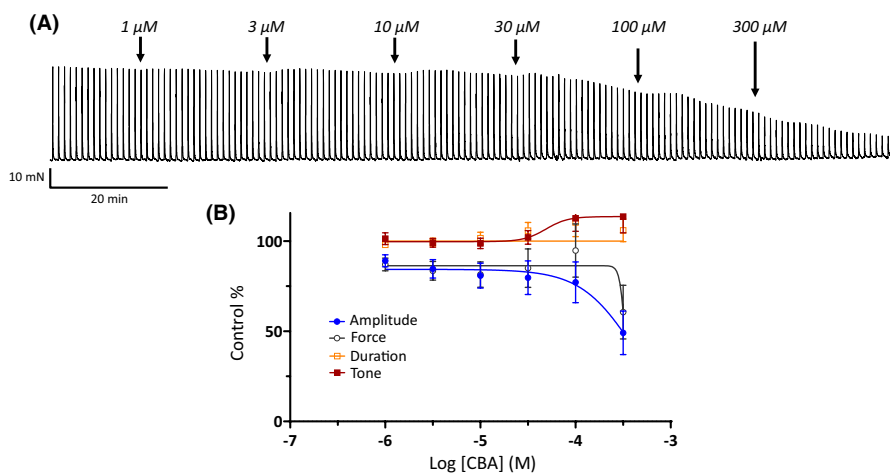


**FIGURE 3** Weak potency of CBA on nerve-evoked UBSM contractions. (A) Shown is a representative isometric UBSM tension recording demonstrating the effect of cumulative additions of CBA (1–300 μM) on nerve-evoked UBSM contractions induced by continuous EFS with 10 Hz stimulation at 1 min intervals. (B) Presented are summary concentration-response graphs for CBA on UBSM nerve-evoked contraction amplitude, muscle force, duration (half-width), and muscle tone ( $n = 11$ ,  $N = 4$ ).

was fully reversible upon washout ( $1.12 \pm 0.16$ ,  $n = 7$ ,  $N = 7$ ). The cell capacitance was not affected by FFA ( $n = 7$ ,  $N = 7$ ; control:  $44.9 \pm 7.7$  pF, FFA:  $45.4 \pm 8.1$  pF,  $p > .05$ , paired Student's *t*-test). To further demonstrate that the specific UBSM cells tested still retained sensitivity to 9-phenanthrol, this widely used inhibitor was subsequently added to the same UBSM cells previously evaluated for FFA following its washout. 9-Phenanthrol effectively

attenuated voltage-step-induced cation currents (Figure 6). In contrast to FFA, 9-phenanthrol increased the cell capacitance in the same cells ( $n = 7$ ,  $N = 7$ ; control:  $44.3 \pm 7.2$  pF, 9-phenanthrol:  $48.3 \pm 7.9$  pF;  $p < .02$ , paired *t*-test). Collectively, voltage-step-induced cation currents, which were robustly blocked by 9-phenanthrol, were not inhibited by FFA; instead, a modest current enhancement occurred.

**FIGURE 4** Lack of an effect by CBA on membrane potential in isolated UBSM cells. (A) Shown is a representative recording for the addition of CBA ( $30\ \mu\text{M}$ ) on the membrane potential measured in a single UBSM cell in current-clamp ( $I = 0$ ) mode. (B) A graph summarizing data for the control and CBA ( $30\ \mu\text{M}$ ) is displayed as individual values with means  $\pm$  SEM ( $n = 7$ ,  $N = 7$ ).

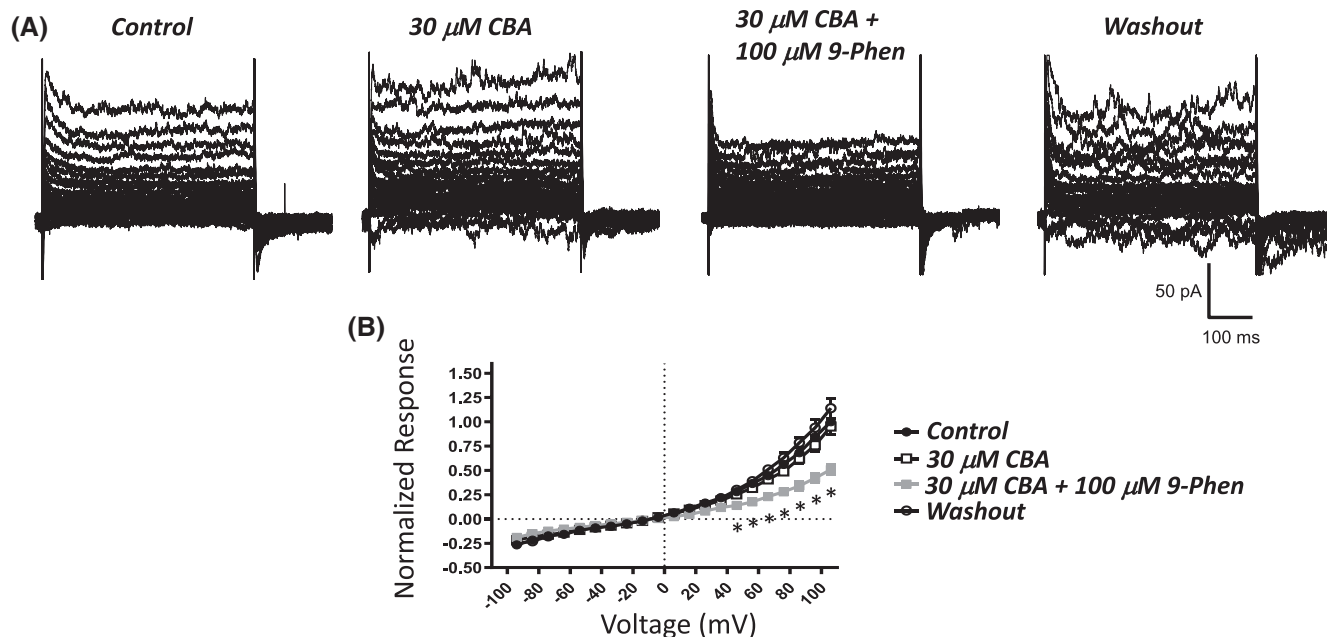
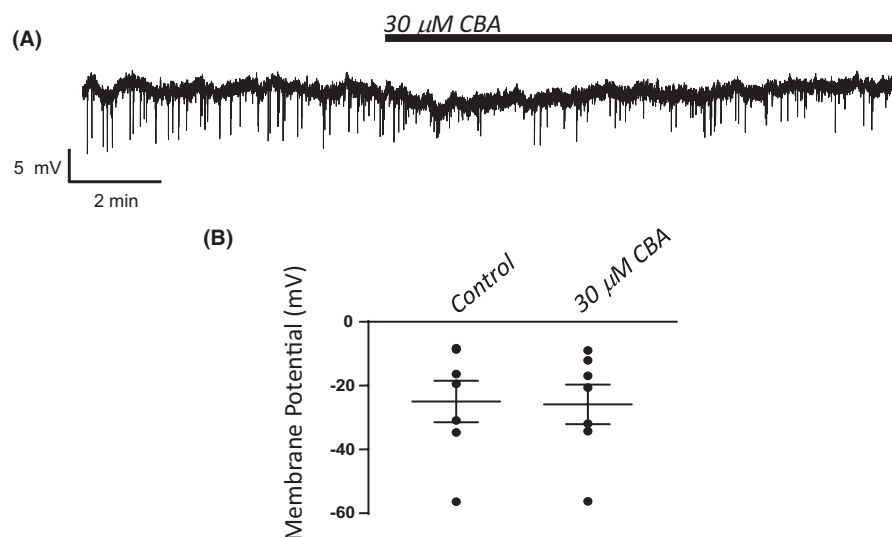


**FIGURE 5** Absence of an inhibitory effect by CBA on voltage step-induced cation currents sensitive to 9-phenanthrol in isolated UBSM cells. (A) Depicted are representative current traces obtained for the control,  $30\ \mu\text{M}$  CBA,  $100\ \mu\text{M}$  9-phenanthrol (9-Phen) added in the presence of CBA, and washout in the same UBSM cell. The UBSM cell was held at  $-74\ \text{mV}$  and stepped to voltages ranging from  $-94$  to  $+106\ \text{mV}$  for  $500\ \text{ms}$  in  $10\ \text{mV}$  increments, and returned to  $-74\ \text{mV}$ . (B) A summary graph illustrating normalized responses for the control,  $30\ \mu\text{M}$  CBA,  $100\ \mu\text{M}$  9-phenanthrol (9-Phen) in the presence of CBA, and after washout ( $n = 3-6$ ,  $N = 3-7$ ). Two-way ANOVA analysis did not reveal a statistically significant interaction for the effects of voltage and the presence of CBA (control versus  $30\ \mu\text{M}$  CBA,  $F[20|100] = 0.0670$ ,  $p = .847$ ). A significant interaction was observed for voltage and the presence or absence of 9-phenanthrol (control versus CBA versus 9-Phen+CBA,  $F[40|160] = 10.24$ ,  $p < .0001$ ); \* indicates significance ( $p < .05$ , Sidak multiple comparison post hoc test) at each voltage for the comparisons of 9-Phen+CBA versus both control and CBA conditions.

### 3.4 | BTP2, a nonselective TRPM4 channel activator, does not increase 9-phenanthrol-sensitive voltage-step-induced cation currents in isolated UBSM cells

Among the various pharmacological effects of BTP2, enhancement of TRPM4 currents has been reported.<sup>27</sup> Here, the effect of BTP2

( $10\ \mu\text{M}$ ) was evaluated on the voltage-step-induced cation currents. BTP2 did not alter the currents (Figure 7). The subsequent addition of 9-phenanthrol in the presence of BTP2 decreased the currents, especially over positive voltages. Under our experimental conditions, significant current inhibitions by 9-phenanthrol in the presence of BTP2 were observed at  $+56\ \text{mV}$  and above. For example, the normalized responses at  $+106\ \text{mV}$  for control, BTP2, and 9-phenanthrol

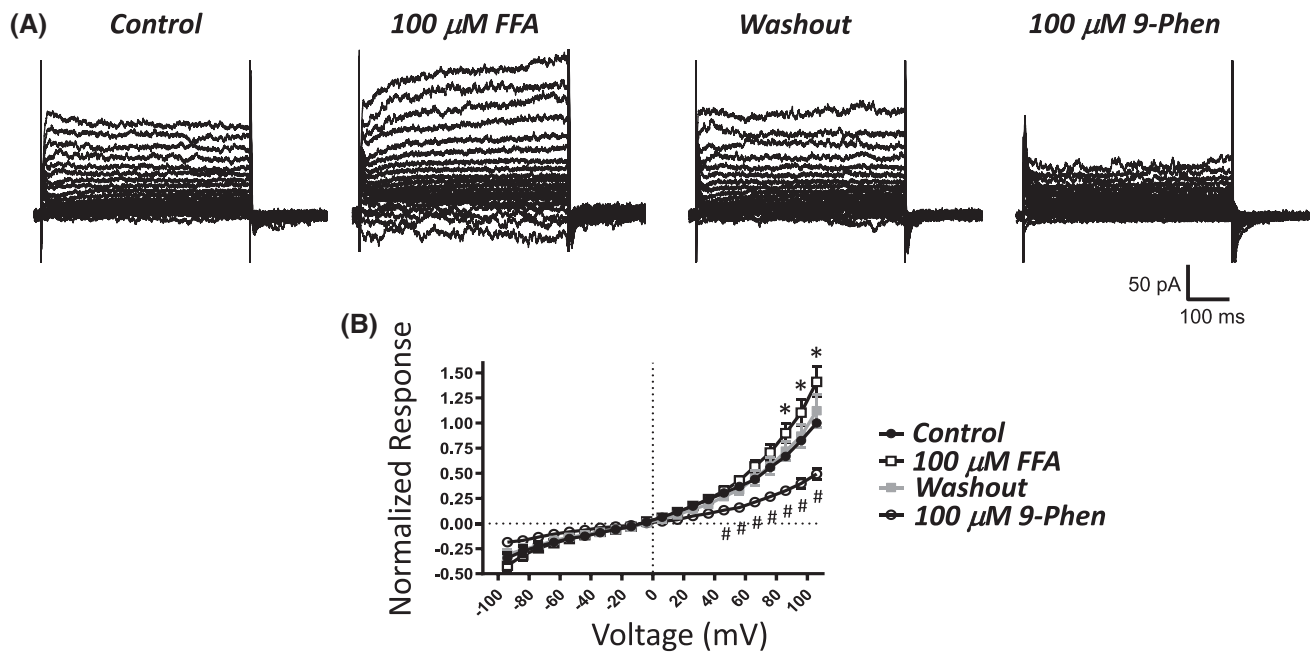


**FIGURE 6** Lack of inhibitory effects of flufenamic acid, a non-selective TRPM4 channel inhibitor, on 9-phenanthrol-sensitive voltage step-induced cation currents in isolated UBSM cells. (A) Depicted are representative current traces obtained for the control, 100 μM flufenamic acid (FFA), washout of FFA/control for 9-phenanthrol (9-Phen), and 100 μM 9-Phen in the same UBSM cell. The UBSM cell was held at  $-74$  mV and stepped to voltages ranging from  $-94$  to  $+106$  mV for 500 ms in 10 mV increments, and returned to  $-74$  mV. (B) A summary graph illustrates normalized responses for the control, 100 μM FFA, washout/control, and 100 μM 9-Phen ( $n = 7$ ,  $N = 7$ ). Two-way ANOVA analysis revealed a statistically significant interaction between the effects of voltage and test condition (control vs FFA vs washout/control vs 9-Phen,  $F[60360] = 16.09$ ,  $p < .0001$ ); \* and # indicate significance ( $p < .05$ , Sidak multiple comparison post hoc test) at each voltage for the comparisons of FFA vs control (\*) and 9-Phen vs washout (#).

with BTP2 were  $1.00 \pm 0.10$  ( $n = 6$ ,  $N = 5$ ,  $p > .05$ , Sidak multiple comparison post hoc test), and  $0.54 \pm 0.07$  ( $n = 5$ ,  $N = 4$ ,  $p < .05$ , Sidak multiple comparison post hoc test vs.  $1.02 \pm 0.12$  for matched cells in BTP2), respectively. Hence, 9-phenanthrol-sensitive currents were not affected by BTP2. BTP2 did not change the cell capacitance ( $n = 6$ ,  $N = 5$ , control:  $46.4 \pm 4.2$  pF; BTP2:  $46.3 \pm 4.2$  pF).

### 3.5 | Depolarizing holding potentials do not increase voltage-step-induced cation currents in isolated UBSM cells

A previous study on recombinant and native TRPM4 channels reported that TRPM4 currents display dependency on the holding voltage. The TRPM4 currents show enhancement upon a strong depolarizing holding voltage.<sup>27</sup> Here, the voltage-step-induced currents in UBSM cells were examined at the standard holding voltage  $V_{\text{hold}}$  of  $-74$  mV – as used for all voltage-step experiments reported so far – and compared to those determined at  $V_{\text{hold}}$  of either  $+6$  or  $+26$  mV (Figure 8). Under the recording conditions, the voltage-step-induced currents measured at  $V_{\text{hold}} + 6$  and  $+26$  mV showed reduction, especially for positive voltage steps ( $+46$  to  $+106$  mV), when compared to  $V_{\text{hold}}$  of  $-74$  mV. For instance, for the voltage step to  $+106$  mV under  $V_{\text{hold}}$  of  $-74$ ,  $+6$ , and  $+26$  mV, the normalized responses were, respectively, 1,  $0.78 \pm 0.05$  ( $n = 9$ ,  $N = 6$ ,  $p < .05$ ,

Sidak multiple comparison post hoc test),  $0.78 \pm 0.05$  ( $n = 9$ ,  $N = 6$ ,  $p < .05$ , Sidak multiple comparison post hoc test). These experiments illustrate that in UBSM cells voltage-step-induced cation currents show a degree of voltage-sensitivity based on  $V_{\text{hold}}$ ; depolarizing  $V_{\text{hold}}$  conditions promote reduction in the voltage-step-induced currents. Cell capacitance was the same for all three  $V_{\text{hold}}$  conditions ( $48.7 \pm 4.1$  pF for  $V_{\text{hold}}$  of  $-74$  mV,  $+6$  mV, and  $+26$  mV;  $n = 9$ ,  $N = 6$ ).

## 4 | DISCUSSION

The role of TRPM4 channels in UBSM function is primarily interpreted from the inhibitory effects of 9-phenanthrol, a widely used blocker. Here, we examined whether CBA, a novel and potent TRPM4 channel inhibitor,<sup>20,34</sup> could also reduce guinea pig excitability and contractility. Unlike 9-phenanthrol, CBA displayed either no or weak inhibitory effects on UBSM contractions. In UBSM cells, CBA (30 μM) failed to replicate UBSM hyperpolarization and attenuation of voltage-step cation currents observed for 9-phenanthrol (this study and<sup>3</sup>). The TRPM4 channel inhibitor FFA<sup>20,26,33</sup> and the activator BTP2,<sup>27,35</sup> did not alter the UBSM voltage-step whole-cell-induced currents as expected via TRPM4 channel interaction. Collectively, TRPM4 channels in guinea pig UBSM, although expressed at the protein level,<sup>3,13</sup> likely determine a function distinct from excitation-contraction regulation.



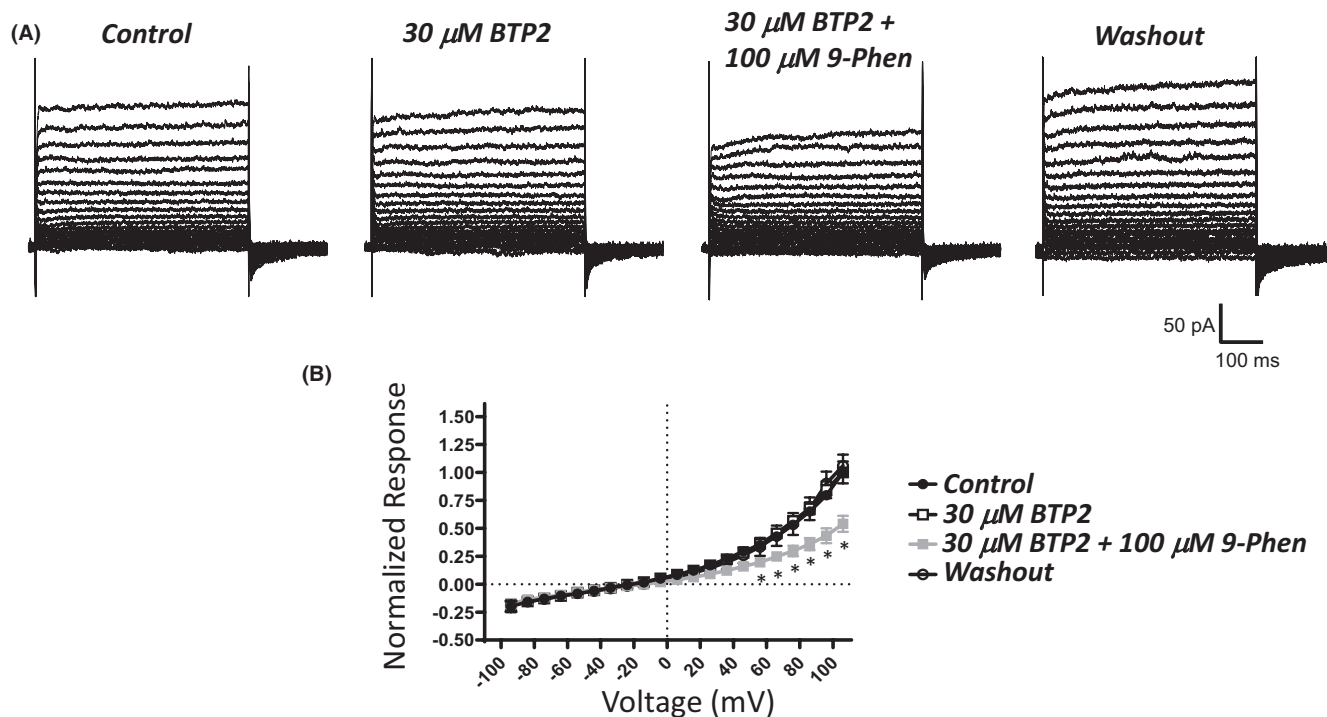


**FIGURE 7** No BTP2-induced changes in 9-phenanthrol-sensitive voltage step-induced cation currents in UBSM cells. (A) Displayed are representative current traces obtained for the control, 30 μM BTP2 (or YM-58483), 100 μM 9-phenanthrol (9-Phen) added in the presence of BTP2, and after washout in the same UBSM cell. The UBSM cell was held at  $-74$  mV and stepped to voltages ranging from  $-94$  to  $+106$  mV for 500 ms in 10 mV increments, and returned to  $-74$  mV. (B) A summary graph illustrates normalized responses for the control, 30 μM BTP2, 100 μM 9-Phen in the presence of BTP2, and after washout ( $n = 3-6$ ,  $N = 3-5$ ). Two-way ANOVA analysis did not reveal a statistically significant interaction for the effects of voltage and the presence of BTP2 (control versus 30 μM BTP2,  $F[20100] = 0.176$ ,  $p > .9999$ ). A significant interaction was observed for voltage and the presence or absence of 9-Phen (control versus CBA versus 9-Phen+BTP2,  $F[40160] = 10.24$ ,  $p < .0001$ ); \* indicates significance ( $p < .05$ , Sidak multiple comparison post hoc test) at each voltage for the comparisons of 9-Phen+BTP2 versus both control and BTP2 conditions.

CBA displays ~3- to 10-fold higher potency than 9-phenanthrol, but comparable maximum efficacy on recombinant TRPM4 currents.<sup>20</sup> We hypothesized that CBA would be more potent than 9-phenanthrol in inhibiting UBSM contractions. Instead, CBA displayed either no or weak inhibition on spontaneous, 20 mM KCl-induced, and EFS-induced contractions (Figures 1-3). The modest CBA-induced inhibition observed at the highest concentrations likely reflects non-selectivity.<sup>36</sup> In contrast, 9-phenanthrol strongly inhibited guinea pig UBSM contractility.<sup>3,13,15</sup> In our experiments, the maximum concentration of DMSO to dissolve CBA was 0.3% (v/v). At this concentration, the vehicle exhibits only modest effects on guinea pig UBSM contractility specifically increases up to 30% on the amplitude and muscle force and no significant effects on other contraction parameters that were associated with ~20% reduction in the tone.<sup>15</sup> The effects of CBA and 9-phenanthrol are, hence, distinct from the vehicle. CBA failed to alter the membrane potential and the voltage-step-induced currents (Figures 4-5). In comparison, 9-phenanthrol-induced hyperpolarization and attenuated the voltage-step-induced currents.<sup>3,15</sup> CBA, hence, did not mimic the inhibitory effects of 9-phenanthrol in guinea pig UBSM.

Several causes may underlie differences in the effects of 9-phenanthrol and CBA. First, 9-phenanthrol mediated effects could be due to non-TRPM4 channel pharmacology. 9-Phenanthrol is not very selective for TRPM4 channels as this compound also acts on TMEM16A/Ano1  $Cl^-$ ,  $Ca_v$ ,  $Na_v$ ,  $K_v$ , and IK channels and induces cytotoxicity.<sup>21-25</sup> In UBSM cells, 9-phenanthrol also increased cell capacitance, an effect independent of TRPM4 channel involvement.<sup>15</sup> Unlike 9-phenanthrol, the novel TRPM4 channel blocker CBA<sup>20,34</sup> and the activator BTP2<sup>27,35</sup> did not change the voltage-step-induced cation currents in UBSM cells (Figures 5 and 7). FFA, another non-selective TRPM4 channel blocker,<sup>20,26,33</sup> did not attenuate the currents but induced either no change or increase at very positive voltages (Figure 8). The enhancing effect of FFA may be due to the activation of TRPA1 channels.<sup>37</sup> Among the tested TRPM4 channel modulators only 9-phenanthrol displayed robust inhibitory efficacy on UBSM electrical and mechanical activities. Second, differential effects of 9-phenanthrol and CBA may be potentially explained by species differences. At present, the full sequence of the guinea pig TRPM4 channel has not yet been cloned, precluding its expression and thus investigation. In contrast, both 9-phenanthrol and CBA fully blocked recombinant human TRPM4 channels when

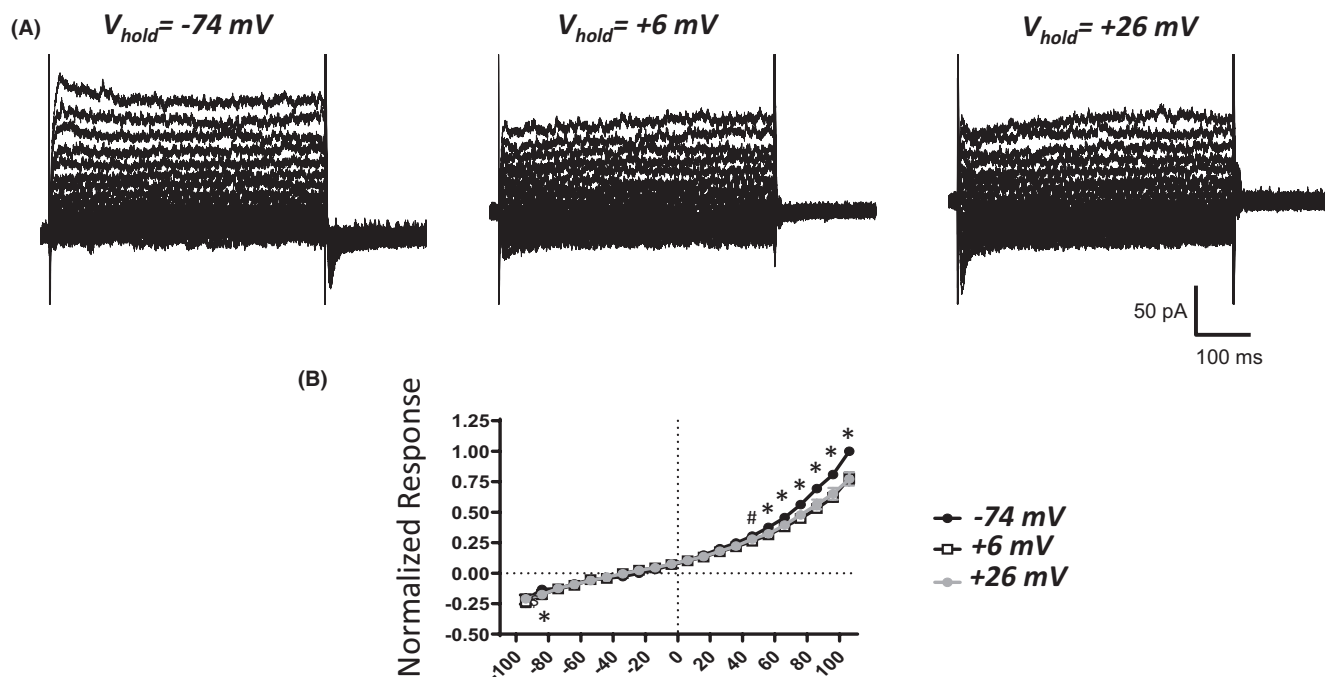


**FIGURE 8** Lack of increase in voltage step-induced cation currents with depolarizing holding potentials in isolated UBSM cells. (A) Shown are representative voltage-step-induced cation currents measured with the standard voltage step protocol (10 mV voltage step increments with 500 ms duration from  $-94$  mV to  $+106$  mV) at three different test holding potentials ( $V_{hold}$ ) of  $-74$  mV,  $+6$  mV, and  $+26$  mV in the same UBSM cell. (B) Summary graph displaying normalized responses versus voltage for the three test holding potentials ( $-74$  mV,  $+6$  mV, and  $+26$  mV) obtained in UBSM cells [ $n = 9$ ,  $N = 6$ ]. Two-way ANOVA analysis showed a significant interaction for the effects of voltage step value and test holding potential variable ( $-74$  mV versus  $+6$  mV versus  $+26$  mV,  $F[40, 320] = 11.04$ ,  $p < .0001$ ); \* and # indicate significance (Sidak multiple comparison post hoc test) at each voltage for  $-74$  mV versus both  $+6$  mV and  $+26$  mV (\*), and  $-74$  mV versus  $+6$  mV (#).

expressed in HEK293 and tsa201 cells.<sup>20,21</sup> For mouse TRPM4 channels, contradictory findings exist. CBA in excised patches of mouse recombinant TRPM4 channels either did not affect the cation currents or caused potentiation when applied extracellularly or intracellularly, respectively.<sup>21</sup> 9-Phenanthrol applied extracellularly but not intracellularly blocked TRPM4 currents.<sup>21</sup> This orientation-specificity for 9-phenanthrol was surprising given high hydrophobicity of 9-phenanthrol (xLogP of 3.6, see PubChem), and the ease with which it is expected to cross the cell membrane. Conversely, native mouse TRPM4 currents in pancreatic acinar cells were inhibited by CBA and 9-phenanthrol.<sup>38</sup> Future studies are needed to establish how CBA affects mouse and guinea pig TRPM4 channels. Third, TRPM4 channels in UBSM exist in a configuration state regardless of species that exhibit a unique pharmacological profile: sensitivity to 9-phenanthrol, insensitivity to CBA and FFA, and only partial inhibition by glibenclamide, another non-selective TRPM4 channel blocker.<sup>15</sup> Among these explanations, we favor the first that the effects of 9-phenanthrol in UBSM are due to a non-TRPM4 channel interaction.

Other confounding factors in our electrophysiological experiments are the temperature-dependency of TRPM4 channels and dependency on intracellular  $Ca^{2+}$ .<sup>39</sup> Half voltage activation constant for TRPM4 currents shifted  $\sim -50$  mV when changed from 20 to 31°C, and the channel opening required high  $Ca^{2+}$

( $>10$ – $100$   $\mu$ M).<sup>39</sup> Our electrophysiological recordings were conducted at room temperature and under condition where intracellular  $Ca^{2+}$  levels could not be controlled experimentally. We acknowledge these limitations. TRPM4 currents, however, have been recorded in cerebral vascular smooth muscle cells using the same experimental approach as utilized here.<sup>40,41</sup> Recombinant TRPM4 currents have been routinely measured at room temperature.<sup>9,20</sup> If temperature played a role, then there should have been a discrepancy observed between electrophysiological and contractile responses for CBA measured, respectively, at  $\sim 22^\circ$ C and  $37^\circ$ C. This was not observed. CBA lacked robust inhibitory responses. Contraction experiments also illuminate the issue of elevated intracellular  $Ca^{2+}$ . Both 20 mM KCl-induced contractions and EFS-induced contractions elevate intracellular  $Ca^{2+}$  levels, and yet CBA efficacy remained comparable and weak for all three contractility protocols (Figures 1–3). Of note, for 20 mM KCl-induced contractions, we observed an enhancement in the frequency for the highest CBA concentrations, most likely due to non-selectivity. As CBA has been recently shown to inhibit transient outward  $K^+$  current and late  $Na^+$  current in ventricular myocytes,<sup>36</sup> this compound may lack optimal selectivity.

Given the issues with the currently available TRPM4 channel pharmacological tools, determining the roles of TRPM4 channel function in UBSM will require additional approaches. The utility

of genetic animal models, whether global or inducible conditional, will be extremely useful as has been the case for elucidating the roles of TRPM4 channels in the heart, taste buds, brain, and pancreas.<sup>38,42-46</sup> Unfortunately, the specific TRPM4 knockout mouse or rat strains have not yet been made available to us. We look forward to these prospective studies providing further insights.

As TRPM4 channels are robustly expressed in UBSM cells and tissues of humans, rats, guinea pigs, and mice,<sup>3-5,7,12</sup> a question arises as to their overall physiological role in the urinary bladder. Our current study provides evidence that they may not directly regulate UBSM excitability or contractility. For non-smooth muscle cells, TRPM4 channels have been implicated in the regulation of hypertrophy, cell growth, proliferation, migration, and cell differentiation promoting fibrosis.<sup>45,47-49</sup> Additionally, TRPM4 channels form interacting complexes with TRPC3 and SUR1 subunits as well as cytoskeletal adhesion proteins affecting their properties,<sup>50-52</sup> although in healthy UBSM cells TRPM4-SUR1 complexes are unlikely to be functional.<sup>15</sup> TRPM4 channels may play one of these roles in UBSM cells. A recent report found a time-dependent upregulation of TRPM4 channel expression in the bladder of a spinal cord injury mouse model suggesting a contribution of TRPM4 channels to post-injury healing.<sup>7</sup> TRPM4 channel protein expression also changed during maturation from youth to adulthood in guinea pigs for both intracellular and cell surface expression perhaps related to the putative non-excitatory, non-contractile regulatory role.<sup>13</sup> Additional mechanistic studies are, therefore, needed to unravel the functional role of TRPM4 channels in UBSM.

In summary, the novel TRPM4 channel inhibitor CBA did not mimic the inhibitory effects of the classical and non-selective inhibitor 9-phenanthrol on UBSM electrical and mechanical activities. Two other TRPM4 channel modulators FFA and BTP2 did not affect UBSM cation currents as expected for the TRPM4 channel engagement. Our study, hence, suggests that TRPM4 channels, although expressed in UBSM, play an additional role (e.g., in cell proliferation or under pathophysiological conditions) rather than regulation of excitability and contractility.

#### AUTHOR CONTRIBUTIONS

*Participated in research design:* Malysz, Maxwell, and Petkov. *Conducted experiments:* Malysz and Maxwell. *Performed data analyses:* Malysz and Maxwell. *Wrote or contributed to the writing of the manuscript:* Malysz, Maxwell, and Petkov.

#### ACKNOWLEDGMENTS

The authors thank Mr. Todor B. Gasharov for technical assistance with some of the experiments and Dr. Wenkuan Xin for providing critical comments that helped to improve the content of our paper.

This publication was supported by the National Institute of Diabetes and Digestive and Kidney Diseases under Award Numbers R01 DK-106964 and P20 DK-123971. The content is solely the responsibility of the authors and does not necessarily represent the official views of the National Institutes of Health.

#### FUNDING INFORMATION

This publication was supported by the National Institute of Diabetes and Digestive and Kidney Diseases under Award Numbers R01 DK-106964 and P20 DK-123971. The content is solely the responsibility of the authors and does not necessarily represent the official views of the National Institutes of Health.

#### DISCLOSURE

The authors declare no conflict of interest.

#### DATA AVAILABILITY STATEMENT

The data supporting the findings of this study are available from the corresponding authors upon request.

#### ETHICS STATEMENT

Experiments were conducted in accordance with the Animal Use Protocols Nos. 17-075 and 20-019 reviewed and approved by the University of Tennessee Health Science Center (Memphis, TN).

#### ORCID

John Malysz  <https://orcid.org/0000-0001-7012-8200>

Sarah E. Maxwell  <https://orcid.org/0000-0003-3427-4846>

Georgi V. Petkov  <https://orcid.org/0000-0001-6471-1803>

#### REFERENCES

- Andersson KE, Arner A. Urinary bladder contraction and relaxation: physiology and pathophysiology. *Physiol Rev.* 2004;84:935-986.
- Malysz J, Petkov GV. Urinary bladder smooth muscle ion channels: expression, function, and regulation in health and disease. *Am J Physiol Renal Physiol.* 2020;319:F257-F283.
- Smith AC, Hristov KL, Cheng Q, et al. Novel role for the transient potential receptor melastatin 4 channel in Guinea pig detrusor smooth muscle physiology. *Am J Physiol Cell Physiol.* 2013;304:C467-C477.
- Smith AC, Parajuli SP, Hristov KL, et al. TRPM4 channel: a new player in urinary bladder smooth muscle function in rats. *Am J Physiol Renal Physiol.* 2013;304:F918-F929.
- Hristov KL, Smith AC, Parajuli SP, Malysz J, Rovner ES, Petkov GV. Novel regulatory mechanism in human urinary bladder: central role of transient receptor potential melastatin 4 channels in detrusor smooth muscle function. *Am J Physiol Cell Physiol.* 2016;310:C600-C611.
- Alom F, Matsuyama H, Nagano H, Fujikawa S, Tanahashi Y, Unno T. Involvement of transient receptor potential melastatin 4 channels in the resting membrane potential setting and cholinergic contractile responses in mouse detrusor and ileal smooth muscles. *J Vet Med Sci.* 2019;81:217-228.
- Kullmann FA, Beckel JM, McDonnell B, et al. Involvement of TRPM4 in detrusor overactivity following spinal cord transection in mice. *Naunyn Schmiedebergs Arch Pharmacol.* 2018;391:1191-1202.
- Nilius B, Owsianik G. The transient receptor potential family of ion channels. *Genome Biol.* 2011;12:218.
- Nilius B, Prenen J, Droogmans G, et al. Voltage dependence of the Ca<sup>2+</sup>-activated cation channel TRPM4. *J Biol Chem.* 2003;278:30813-30820.
- Wang C, Naruse K, Takahashi K. Role of the TRPM4 channel in cardiovascular physiology and pathophysiology. *Cell.* 2018;7:E62.
- Earley S. TRPM4 channels in smooth muscle function. *Pflugers Arch.* 2013;465:1223-1231.

12. Parajuli SP, Hristov KL, Sullivan MN, et al. Control of urinary bladder smooth muscle excitability by the TRPM4 channel modulator 9-phenanthrol. *Channels (Austin)*. 2013;7:537-540.
13. Maxwell SE, Leo MD, Malysz J, Petkov GV. Age-dependent decrease in TRPM4 channel expression but not trafficking alters urinary bladder smooth muscle contractility. *Physiol Rep*. 2021;9:e14754.
14. Guinamad R, Hof T, Del Negro CA. The TRPM4 channel inhibitor 9-phenanthrol. *Br J Pharmacol*. 2014;171:1600-1613.
15. Malysz J, Maxwell SE, Yarotsky V, Petkov GV. TRPM4 channel inhibitors 9-phenanthrol and glibenclamide differentially decrease Guinea pig detrusor smooth muscle whole-cell cation currents and phasic contractions. *Am J Physiol Cell Physiol*. 2020;318:C406-C421.
16. Barbet G, Demion M, Moura IC, et al. The calcium-activated nonselective cation channel TRPM4 is essential for the migration but not the maturation of dendritic cells. *Nat Immunol*. 2008;9:1148-1156.
17. Cheng H, Beck A, Launay P, et al. TRPM4 controls insulin secretion in pancreatic beta-cells. *Cell Calcium*. 2007;41:51-61.
18. Serafini N, Dahdah A, Barbet G, et al. The TRPM4 channel controls monocyte and macrophage, but not neutrophil, function for survival in sepsis. *J Immunol*. 2012;189:3689-3699.
19. Grand T, Demion M, Norez C, et al. 9-phenanthrol inhibits human TRPM4 but not TRPM5 cationic channels. *Br J Pharmacol*. 2008;153:1697-1705.
20. Ozhatil LC, Delalande C, Bianchi B, et al. Identification of potent and selective small molecule inhibitors of the cation channel TRPM4. *Br J Pharmacol*. 2018;175:2504-2519.
21. Arullampalam P, Preti B, Ross-Kaschitzka D, Lochner M, Rougier JS, Abriel H. Species-specific effects of cation channel TRPM4 small-molecule inhibitors. *Front Pharmacol*. 2021;12:712354.
22. Burris SK, Wang Q, Bulley S, Neeb ZP, Jaggar JH. 9-phenanthrol inhibits recombinant and arterial myocyte TMEM16A channels. *Br J Pharmacol*. 2015;172:2459-2468.
23. Hou JW, Fei YD, Li W, et al. The transient receptor potential melastatin 4 channel inhibitor 9-phenanthrol modulates cardiac sodium channel. *Br J Pharmacol*. 2018;175:4325-4337.
24. Simard C, Salle L, Rouet R, Guinamad R. Transient receptor potential melastatin 4 inhibitor 9-phenanthrol abolishes arrhythmias induced by hypoxia and re-oxygenation in mouse ventricle. *Br J Pharmacol*. 2012;165:2354-2364.
25. Veress R, Baranyai D, Hegyi B, et al. Transient receptor potential melastatin 4 channel inhibitor 9-phenanthrol inhibits K<sup>+</sup> but not Ca<sup>2+</sup> currents in canine ventricular myocytes. *Can J Physiol Pharmacol*. 2018;96:1022-1029.
26. Amarouch MY, Syam N, Abriel H. Biochemical, single-channel, whole-cell patch clamp, and pharmacological analyses of endogenous TRPM4 channels in HEK293 cells. *Neurosci Lett*. 2013;541:105-110.
27. Takezawa R, Cheng H, Beck A, et al. A pyrazole derivative potently inhibits lymphocyte Ca<sup>2+</sup> influx and cytokine production by facilitating transient receptor potential melastatin 4 channel activity. *Mol Pharmacol*. 2006;69:1413-1420.
28. Malysz J, Rovner ES, Wake R, Petkov GV. Preparation and utilization of freshly isolated human detrusor smooth muscle cells for characterization of 9-phenanthrol-sensitive cation currents. *J Vis Exp*. 2020. doi: 10.3791/59884
29. Malysz J, Buckner SA, Daza AV, Milicic I, Perez-Medrano A, Gopalakrishnan M. Functional characterization of large conductance calcium-activated K<sup>+</sup> channel openers in bladder and vascular smooth muscle. *Naunyn Schmiedebergs Arch Pharmacol*. 2004;369:481-489.
30. Shiga KI, Hirano K, Nishimura J, Niuro N, Naito S, Kanaide H. Dimethyl sulphoxide relaxes rabbit detrusor muscle by decreasing the Ca<sup>2+</sup> sensitivity of the contractile apparatus. *Br J Pharmacol*. 2007;151:1014-1024.
31. Harding SD, Sharman JL, Faccenda E, Southan C, Pawson AJ, Ireland S, Gray AJG, Bruce L, Alexander SPH, Anderton S, Bryant C, Davenport AP, Doerig C, Fabbro D, Levi-Schaffer F, Spedding M, Davies JA, NC-IUPHAR (2018). The IUPHAR/BPS guide to pharmacology in 2019: updates and expansion to encompass the new guide to immunopharmacology. *Nucleic Acids Res* 46: D1091-1106. 10.1093/nar/gkx1121
32. Alexander SPH, Kelly E, Mathie A, et al. The concise guide to pharmacology 2019/20: introduction and other protein targets. *Br J Pharmacol*. 2019;176(S1):S1-S10.
33. Constantine M, Liew CK, Lo V, et al. Heterologously-expressed and liposome-reconstituted human transient receptor potential melastatin 4 channel (TRPM4) is a functional tetramer. *Sci Rep*. 2016;6:19352.
34. Delalande C, Awale M, Rubin M, et al. Optimizing TRPM4 inhibitors in the MHFP6 chemical space. *Eur J Med Chem*. 2019;166:167-177.
35. Riquelme D, Silva I, Philp AM, et al. Subcellular localization and activity of TRPM4 in medial prefrontal cortex layer 2/3. *Front Cell Neurosci*. 2018;12:12.
36. Dienes C, Hézsó T, Kiss DZ, et al. Electrophysiological effects of the transient receptor potential melastatin 4 channel inhibitor (4-chloro-2-[2-chlorophenoxy]acetamido)benzoic acid (CBA) in canine left ventricular cardiomyocytes. *Int J Mol Sci*. 2021;22:9499.
37. Hu H, Tian J, Zhu Y, et al. Activation of TRPA1 channels by fenamate nonsteroidal anti-inflammatory drugs. *Pflugers Arch*. 2010;459:579-592.
38. Diszhazi G, Magyar ZE, Lisztes E, et al. TRPM4 links calcium signaling to membrane potential in pancreatic acinar cells. *J Biol Chem*. 2021;297:101015.
39. Talavera K, Yasumatsu K, Voets T, et al. Heat activation of TRPM5 underlies thermal sensitivity of sweet taste. *Nature*. 2005;438:1022-1025.
40. Gonzales AL, Amberg GC, Earley S. Ca<sup>2+</sup> release from the sarcoplasmic reticulum is required for sustained TRPM4 activity in cerebral artery smooth muscle cells. *Am J Physiol Cell Physiol*. 2010;299:C279-C288.
41. Gonzales AL, Earley S. Endogenous cytosolic Ca<sup>2+</sup> buffering is necessary for TRPM4 activity in cerebral artery smooth muscle cells. *Cell Calcium*. 2012;51:82-93.
42. Bovet-Carmona M, Menigoz A, Pinto S, et al. Disentangling the role of TRPM4 in hippocampus-dependent plasticity and learning: an electrophysiological, behavioral and fMRI approach. *Brain Struct Funct*. 2018;223:3557-3576.
43. Demion M, Thireau J, Gueffier M, et al. Trpm4 gene invalidation leads to cardiac hypertrophy and electrophysiological alterations. *PLoS One*. 2014;9:e115256.
44. Dutta Banik D, Martin LE, Freichel M, Torregrossa AM, Medler KF. TRPM4 and TRPM5 are both required for normal signaling in taste receptor cells. *Proc Natl Acad Sci U S A*. 2018;115:E772-E781.
45. Frede W, Medert R, Poth T, et al. TRPM4 modulates right ventricular remodeling under pressure load accompanied with decreased expression level. *J Card Fail*. 2020;26:599-609.
46. Hedon C, Lambert K, Chakouri N, et al. New role of TRPM4 channel in the cardiac excitation-contraction coupling in response to physiological and pathological hypertrophy in mouse. *Prog Biophys Mol Biol*. 2021;159:105-117.
47. Borgstrom A, Peinelt C, Stoklosa P. TRPM4 in cancer-a new potential drug target. *Biomolecules*. 2021;11:229.
48. Simard C, Magaud C, Adjlane R, et al. TRPM4 non-selective cation channel in human atrial fibroblast growth. *Pflugers Arch*. 2020;472:1719-1732.
49. Wang F, Wu P, Gong S, et al. Aberrant TRPM4 expression in MLL-rearranged acute myeloid leukemia and its blockade induces cell cycle arrest via AKT/GLI1/cyclin D1 pathway. *Cell Signal*. 2020;72:109643.

50. Caceres M, Ortiz L, Recabarren T, et al. TRPM4 is a novel component of the adhesome required for focal adhesion disassembly, migration and contractility. *PLoS One*. 2015;10:e0130540.
51. Cho CH, Lee YS, Kim E, Hwang EM, Park JY. Physiological functions of the TRPM4 channels via protein interactions. *BMB Rep*. 2015;48:1-5.
52. Park JY, Hwang EM, Yarishkin O, et al. TRPM4b channel suppresses store-operated  $Ca^{2+}$  entry by a novel protein-protein interaction with the TRPC3 channel. *Biochem Biophys Res Commun*. 2008;368:677-683.

**How to cite this article:** Malysz J, Maxwell SE, Petkov GV. Differential effects of TRPM4 channel inhibitors on Guinea pig urinary bladder smooth muscle excitability and contractility: Novel 4-chloro-2-[2-(2-chloro-phenoxy)-acetylamino]-benzoic acid (CBA) versus classical 9-phenanthrol. *Pharmacol Res Perspect*. 2022;10:e00982. doi: [10.1002/prp2.982](https://doi.org/10.1002/prp2.982)